

Neutron scattering study of ferroelectric $\text{Sn}_2\text{P}_2\text{S}_6$ under pressure

P. Ondrejčovic,¹ M. Kempa,¹ Y. Vysochanskii,² P. Saint-Grégoire,^{3,4} P. Bourges,⁵ K. Z. Rushchanskii,⁶ and J. Hlinka¹

¹*Institute of Physics, Academy of Sciences of the Czech Republic, Na Slovance 2, 18221 Praha 8, Czech Republic*

²*Institute for Solid State Physics and Chemistry, Uzhgorod University 88000, Uzhgorod, Ukraine*

³*ICGM (UMR CNRS No 5253), C2M, 34095 Montpellier Cedex, France*

⁴*Laboratory MIPA, Department of Sciences and Arts, University of Nimes, 30021 NIMES Cedex 01, France*

⁵*Laboratoire Léon Brillouin, Bât 563 CEA Saclay, 91191 Gif sur Yvette Cedex, France*

⁶*Peter Grünberg Institut, Forschungszentrum Jülich GmbH, 52425 Jülich and JARA-FIT, Germany*

(Received 26 August 2012; published 7 December 2012)

Ferroelectric phase transition in the semiconductor $\text{Sn}_2\text{P}_2\text{S}_6$ single crystal has been studied by means of neutron scattering in the pressure-temperature range adjacent to the anticipated tricritical Lifshitz point ($p \approx 0.18$ GPa, $T \approx 296$ K). The observations reveal a direct ferroelectric-paraelectric phase transition in the whole investigated pressure range (0.18–0.6 GPa). These results are in a clear disagreement with phase diagrams assumed in numerous earlier works, according to which a hypothetical intermediate incommensurate phase extends over several or even tens of degrees in the 0.5 GPa pressure range. Temperature dependence of the anisotropic quasielastic diffuse scattering suggests that polarization fluctuations present above T_C are strongly reduced in the ordered phase. Still, the temperature dependence of the $(\bar{2}00)$ Bragg reflection intensity at $p = 0.18$ GPa can be remarkably well modeled assuming the order-parameter amplitude growth according to the power law with logarithmic corrections predicted for a uniaxial ferroelectric transition at the tricritical Lifshitz point.

DOI: 10.1103/PhysRevB.86.224106

PACS number(s): 77.80.B–, 61.44.Fw

I. INTRODUCTION

Ferroelectric substances with a narrow electronic band gap have recently attracted considerable attention due to their potentially interesting thermoelectric,¹ photovoltaic,^{2,3} and other photoactive properties.^{4–7} Uniaxial ferroelectric chalcogenides represent one of the best known families of ferroelectric semiconductors.⁸ In particular, solid solutions of $\text{Sn}_2\text{P}_2\text{S}_6$ and $\text{Sn}_2\text{P}_2\text{Se}_6$ have been recognized as extremely interesting model systems.^{9–18} All of them have an identical parent paraelectric structure at high temperatures ($P2_1/n$) and the same ferroelectric phase at low temperatures (Pn).^{19–21} At ambient pressure, crystals with low Se/S concentration ratio show a direct ferroelectric-paraelectric phase transition, while those of high Se/S concentration exhibit an intermediate incommensurate (IC) phase (see Fig. 1). The IC phase evidenced in Se-rich solutions^{9,20} resembles a periodic array of antiparallel ferroelectric layers with thickness of about 4 nm ($|q_i| \approx 0.08 \text{ \AA}^{-1}$). The lower-temperature phase transition in $\text{Sn}_2\text{P}_2\text{Se}_6$ could be thus narrated as a discontinuous transformation from a strictly regular “ferroelectric nanodomain” arrangement to a structure with usual, macroscopic ferroelectric domains. This situation is known from many other so-called type-II IC ferroelectric systems, such as thiourea, BCCD, NaNO_2 , etc.¹⁰ The peculiarity of the $\text{Sn}_2\text{P}_2(\text{Se}_x\text{S}_{1-x})_6$ solid solution is that here with decreasing value of Se/S concentration x , the temperature range of the intermediate IC phase continuously decreases and finally the paraelectric-IC and IC-ferroelectric phase transition lines join near the so-called Lifshitz point (LP, see Fig. 1) at $x \approx 0.28$ and $T \approx 280$ K. Theoretically, the modulation period should diverge there.^{22–24}

Later, it was predicted that a similar LP could also occur in the temperature-pressure (T - p) phase diagram of the pure $\text{Sn}_2\text{P}_2\text{S}_6$ crystal. Several experiments indeed confirmed that the phase transition line splits into two lines after crossing the point with coordinates around $p = 0.18$ GPa, $T = 296$ K. The

pure $\text{Sn}_2\text{P}_2\text{S}_6$ system is obviously even more attractive than the $x = 0.28$ compound where, in principle, the LP-related phenomena could be obscured by compositional fluctuations inherent to solid solutions. In addition, thermodynamic analysis of various physical quantities indicated that the Landau free-energy expansion coefficient of the fourth-order term in polarization strongly decreases with pressure in $\text{Sn}_2\text{P}_2\text{S}_6$.⁹ In fact, the thermodynamic coordinates of the tricritical point (TCP), at which this quadratic term vanishes, were predicted to fall in the vicinity of the above discussed LP. This suggests that the fortunate intersection of two special lines—the line of the TCPs and the line of LPs, known also as a tricritical Lifshitz point (TCLP)—might be reached in $\text{Sn}_2\text{P}_2\text{S}_6$ under hydrostatic pressure.²⁵

However, several conflicting statements were reported about the nature of the high-pressure phase transition of $\text{Sn}_2\text{P}_2\text{S}_6$. In particular, recent analysis of the specific heat anomalies²⁶ supports the earlier guess²⁷ that the conditions for the LP are met at lower pressure than the conditions for the TCP. This means that only the LP is realized in the pressure-temperature phase diagram of $\text{Sn}_2\text{P}_2\text{S}_6$. This scenario was repeatedly assumed in Refs. 28–32 and implies that the special point with coordinates around $p = 0.18$ GPa, $T = 296$ K is of the same nature as the LP in the temperature-concentration diagram of $\text{Sn}_2\text{P}_2(\text{Se}_x\text{S}_{1-x})_6$ solid solution (see Fig. 1). On the contrary, other recent measurements, such as birefringence measurements of Ref. 33 were used to support the original scenario of the canonical theory of Ref. 34: That the observed special point in the T - p diagram of $\text{Sn}_2\text{P}_2\text{S}_6$ is merely a TCP but surely not a LP.³³ Moreover, the absence of the LP in the T - p phase diagram of $\text{Sn}_2\text{P}_2\text{S}_6$ was also inferred from the comparisons with the Blume-Emery-Griffith’s model.³⁵ On the top of that, there is a considerable disagreement about the domain of stability of the high-pressure intermediate phase of $\text{Sn}_2\text{P}_2\text{S}_6$ among various sources.^{26,28,36,37}

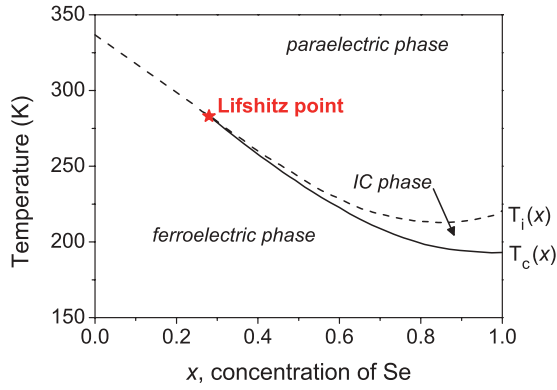


FIG. 1. (Color online) Schematic temperature-composition phase diagram for the system $\text{Sn}_2\text{P}_2(\text{Se}_x\text{S}_{1-x})_6$ according to Refs. 9 and 18. Dashed line is the second-order phase transition and the solid line is the first-order phase transition.

Despite these challenging issues, diffraction investigations of the intermediate phase of $\text{Sn}_2\text{P}_2\text{S}_6$ were not reported so far and there is no direct evidence of its IC nature. The aim of this work is to bring at least a partial answer to the above raised issues by discussion of new results from high-pressure investigations of $\text{Sn}_2\text{P}_2\text{S}_6$ by means of neutron scattering.

II. EXPERIMENTAL DETAILS

The neutron scattering experiment was performed at the Laboratoire Léon Brillouin (Saclay, France) on the 2T1 thermal neutron beam and 4F2 cold neutron beam three-axis spectrometers (TASs). Spectrometers were operated with a PG(002) analyzer set to the neutron wave number $k_f = 2.662 \text{ \AA}^{-1}$ and $k_f = 1.48 \text{ \AA}^{-1}$, respectively. The energy resolution at zero-energy transfer was 0.2 and 0.05 THz, the Q resolution was about 0.01 and 0.005 \AA^{-1} on the 2T1 and 4F2 TASs, respectively.

The $\text{Sn}_2\text{P}_2\text{S}_6$ single crystal used in this experiment was grown from melt by the Bridgeman method at Uzhgorod University. The sample ($\approx 0.8 \text{ cm}^3$) was placed in a special helium pressure cell designed for neutron scattering experiments in a temperature range of 20–305 K and under hydrostatic pressures up to about 0.6 GPa.

The crystal was mounted so that the scattering plane matched its crystallographic mirror plane m_y (throughout the paper, we stick to the pseudo-orthorhombic unit cell defined by $a = 9.378 \text{ \AA}$, $b = 7.488 \text{ \AA}$, $c = 6.513 \text{ \AA}$, and $\beta = 91.15^\circ$, as in Ref. 38). This horizontal plane thus also contains ferroelectric polarization direction (at about 10° – 15° out of the a axis). A reasonably accessible part of the reciprocal space in such a scattering geometry is shown in Fig. 2. A rough survey of uncorrected neutron diffraction intensities of main Bragg reflections in $\text{Sn}_2\text{P}_2\text{S}_6$, as detected at $T = 220 \text{ K}$ and $p = 0.6 \text{ GPa}$ in our experiment, is indicated by variably sized symbols in Fig. 2(a). Results agree fairly well with the neutron diffraction intensities calculated from structural data of the ambient-pressure paraelectric phase of $\text{Sn}_2\text{P}_2\text{S}_6$ [Fig. 2(b), data at $T = 383 \text{ K}$ of Ref. 39].

The a^*c^* plane of Fig. 2 is the same a^*c^* plane within which the satellite reflections with a modulation wave vector $\mathbf{q}_i \approx 0.085\mathbf{c}^* - 0.01\mathbf{a}^*$, demonstrating the IC phase, were observed

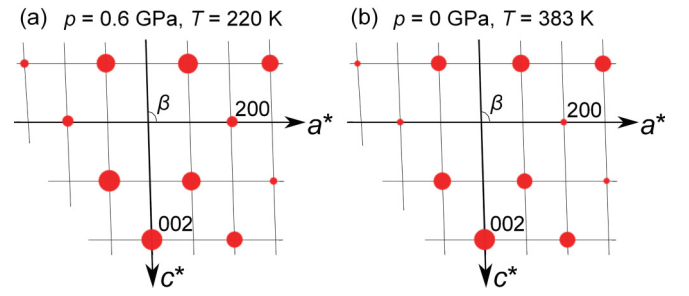


FIG. 2. (Color online) Accessible part of the a^*c^* scattering plane with schematic representation of neutron scattering intensities of principal Bragg reflections in the paraelectric phase. The areas of the circles are proportional to absolute values of neutron scattering structure factors (a) in the present experiment at $p = 0.6 \text{ GPa}$ and $T = 220 \text{ K}$ and (b) $p = 0 \text{ GPa}$ and $T = 383 \text{ K}$ values recalculated from the x-ray data of Ref. 39 using the Jana2006 computer program⁴² with the neutron wave number set to $k_f = 1.48 \text{ \AA}^{-1}$.

in the $\text{Sn}_2\text{P}_2\text{S}_6$ crystal.²⁰ Independent x-ray and neutron scattering experiments^{40,41} agree that satellite reflections of $\text{Sn}_2\text{P}_2\text{S}_6$ are particularly strong for large momentum transfers \mathbf{Q} , roughly parallel to the spontaneous polarization ($\mathbf{Q} \parallel \mathbf{P}_s$). This is a consequence of the usual situation caused by the transverse character of the frozen polarization wave ($\mathbf{q}_i \perp \mathbf{P}_s$), and the same can be anticipated for the supposed $\text{Sn}_2\text{P}_2\text{S}_6$ satellite reflections. Clearly, detection of satellites with a very small modulation wave vector, comparable to the tails of the Q resolution of the instrument, could be problematic in the vicinity of a strong Bragg reflection. Unfortunately, systematic absences are common to both main and satellite reflections, that is, the satellites are expected only around the allowed reflections in the a^*c^* plane. For this reason, most of our measurements were taken in the vicinity of the $(\bar{2}00)$ Bragg reflection. This is an allowed reflection, but rather a weak one, and at the same time the corresponding scattering vector \mathbf{Q} is almost parallel to \mathbf{P}_s .

III. RESULTS

In agreement with our anticipation, the neutron diffraction intensity of the $(\bar{2}00)$ Bragg reflection in the paraelectric phase was several times smaller than in the ferroelectric phase at ambient conditions. In fact, monitoring of the $(\bar{2}00)$ reflection allowed us to probe quite accurately the ferroelectric order parameter. As an example, the temperature dependence of the $(\bar{2}00)$ Bragg reflection intensity at 0.18 and 0.6 GPa is shown in Figs. 3(a) and 3(b). The intensity visibly starts to rise at a well defined temperature that can be associated with the ferroelectric phase transition. The temperatures thus obtained are given in Table I and within the possible experimental error in the pressure and temperature determination they correspond well to those derived from the compressibility anomalies reported in Ref. 28.

In the vicinity of these transition temperatures, we have searched for possible indications of a satellite reflection. The pressure of 0.18 GPa is supposedly that of the TCLP, while the measurements at 0.3 and 0.6 GPa are taken in the region where a finite temperature range of the IC phase was

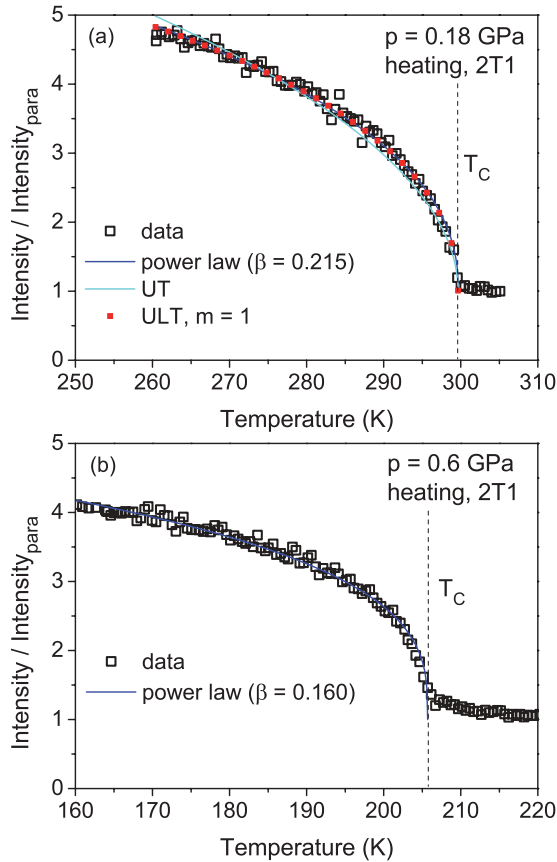


FIG. 3. (Color online) Temperature dependence of the $(\bar{2}00)$ reflection intensity (a) at 0.18 GPa and (b) at 0.6 GPa. The full points and solid lines refer to the fits using Eqs. (4) and (5) with and without logarithmic corrections, respectively.

anticipated. For example, we have recorded intensity maps in a 2D area around the $(\bar{2}00)$ Bragg reflection, extending up to ± 0.2 r.l.u. along both a^* and c^* at 0.6 GPa and temperatures of 205.5, 206, and 206.5 K (at 0.2, 0.7, and 1.2 K above $T_C = 205.3$ K) and similar maps were recorded also at 0.3 GPa and temperatures 267, 270, 273, and 276 K ($T_C = 271$ K). However, no obvious satellite peaks have been seen.

At the same time, our observations disclosed traces of weak and broad diffuse scattering ridges, extending over the “soft” direction, roughly perpendicular to the direction along which the spontaneous polarization is formed. Figure 4(a) shows an example of a scan taken along this diffuse scattering ridge at several temperatures. Examples of transverse scans are shown in Fig. 4(b). Trajectories of these scans are schematically

TABLE I. Phase transition temperatures and β parameters of formulas (4) and (5) without any logarithmic correction for the $(\bar{2}00)$ Bragg reflection measured at given pressure p in the ferroelectric phase on the 2T1 TAS.

| p (GPa) | T_C (K) | β | Heating rate (K/min) |
|-----------|-----------|---------|----------------------|
| 0.18 | 299.6 | 0.215 | 0.22 |
| 0.3 | 271.0 | 0.196 | 0.06 |
| 0.6 | 205.3 | 0.160 | 0.22 |

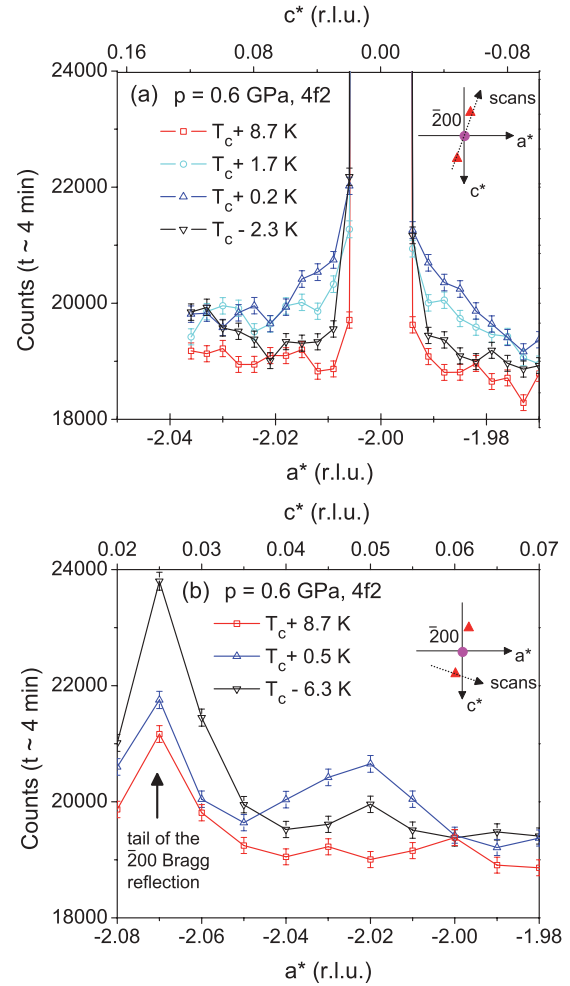


FIG. 4. (Color online) Zero-energy-transfer scans in the $(\bar{2}00)$ Brillouin zone of the $\text{Sn}_2\text{P}_2\text{S}_6$ crystal taken in the vicinity of the ferroelectric phase transition (at 0.6 GPa; near $T_C = 205.3$ K). (a) Scans in the $[-0.03, 0, 1]$ direction (approximately along the diffuse streak), and (b) scans in the $[1, 0, 0.05]$ direction (across the diffuse streak). Measured scan trajectories are schematically indicated in the insets. Solid lines are just guides for the eye.

shown in Fig. 5, along with the contour plots of the ambient-pressure diffuse scattering topography taken from Ref. 43. Note that the diffuse scattering ridge corresponds to the smaller peak in Fig. 4(b), while the larger intensity peak is merely a spurious leakage of $(\bar{2}00)$ Bragg reflection scattering due to the strongly anisotropic tails of the instrumental resolution function.

Some of the scans displayed in Fig. 4(a) show a nonmonotonic intensity decay with the distance from the Brillouin zone center. However, due to the considerable background intensity caused by high-pressure-cell environment, this can hardly be considered as a significant indication of incommensurate satellite reflections. Rather, the anisotropy of this diffuse scattering is obvious and strikingly similar to the critical fluctuations previously seen by x-ray scattering at ambient pressure conditions.⁴³ The assignment of the diffuse scattering to the order-parameter fluctuations is further corroborated by the observed increase of its intensity as the transition is approached from above and by its rather abrupt reduction just

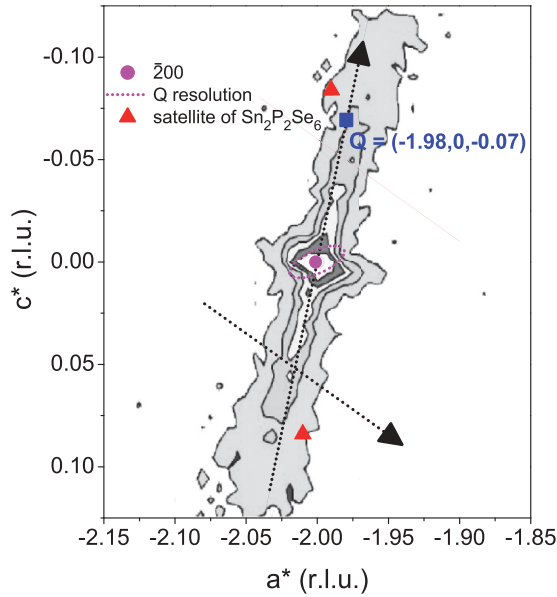


FIG. 5. (Color online) Schema of reciprocal-space trajectories of data scans shown in Fig. 4, superposed with contour plots of the critical diffuse scattering known from ambient pressure x-ray diffraction measurements of Ref. 43. Full triangles indicate positions of incommensurate satellite reflections of the ambient-pressure incommensurate phase of the related compound $\text{Sn}_2\text{P}_2\text{Se}_6$, as reported in Ref. 20.

below the phase transition point [see full points in Fig. 6(b)]. Moreover, few constant-Q spectra taken at selected positions in the high-temperature phase [Fig. 6(a)] suggest that this diffuse scattering is quasielastic in its nature, with FWHM of the order of 0.2 THz. It will be shown in the next section that several important conclusions can be drawn from such measurements, even though the high elastic and inelastic scattering background did not allow their more quantitative analysis.

IV. DISCUSSION

A. Absence of the TCLP, three alternative scenarios

Summarizing, our results do not provide any support for the LP in the T - p phase diagram of $\text{Sn}_2\text{P}_2\text{S}_6$ up to the hydrostatic pressure values of about 0.6 GPa. Thus, the most natural conclusion seems to be that there is no IC phase in this T - p region at all (“scenario A”). The absence of any clear evidence for the LP in the above displayed observations led us nevertheless to perform detailed and careful comparisons of our results with those of previously reported experiments, which did confirm the presence of the LP. In particular, we have traced the T - p phase diagram of $\text{Sn}_2\text{P}_2\text{S}_6$ (see Fig. 7) according to the reported anomalies in the compressibility data (Ref. 28, circles in Fig. 7) and in the dielectric permittivity data (Ref. 36, triangles in Fig. 7). Both these measurements suggest splitting of the phase transition in $\text{Sn}_2\text{P}_2\text{S}_6$ ($x = 0$) at around $p = 0.18$ GPa, $T = 296$ K, which was naturally interpreted as the expected LP. At the same time, the stability range of the anticipated intermediate phase is markedly different in these

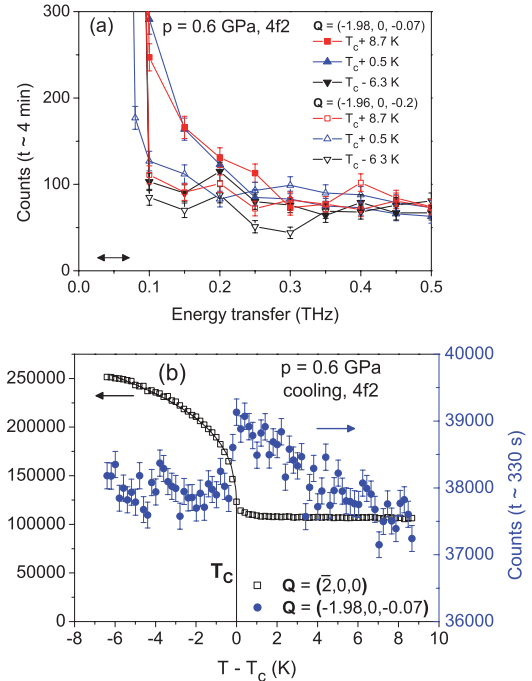


FIG. 6. (Color online) Temperature dependence of both elastic and quasielastic scattering in the $(\bar{2}00)$ Brillouin zone at 0.6 GPa: (a) selected constant-Q scans for several temperatures and (b) principal Bragg reflection intensity at $\mathbf{q} = (0,0,0)$ and elastic diffuse scattering at $\mathbf{q} = (0.02,0,-0.07)$.

two measurements: It opens at the rate of about 190 K/GPa according to Ref. 36 (“scenario B”), while there is only about 20 K/GPa opening rate deduced from measurements of Ref. 28 (“scenario C”).

It is also instructive to compare these data with the T - p phase diagram of the $\text{Sn}_2\text{P}_2\text{S}_6$ crystal, in which the IC phase

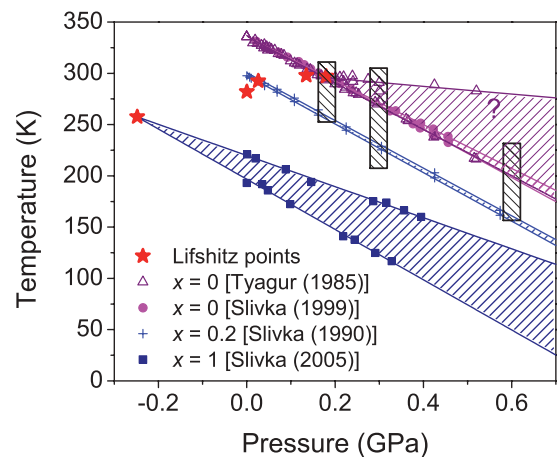


FIG. 7. (Color online) Temperature-pressure phase diagram of $\text{Sn}_2\text{P}_2(\text{Se}_x\text{S}_{1-x})_6$ solid solution. The shaded areas indicate intermediate phases between high-temperature paraelectric and low-temperature ferroelectric phases for given concentrations x . The stars stand for Lifshitz points of solid solution with x equals 1, 0.28, 0.2, 0.04, and 0 (from left to right). Temperature ranges of neutron scattering measurements reported in this work are indicated by vertical rectangular areas.

was firmly established at least at ambient pressure. In fact, the temperature range of the IC phase of $\text{Sn}_2\text{P}_2\text{Se}_6$ (limited by pairs of square symbols in Fig. 7) opens at a rate of about 100 K/GPa, which is just an intermediate value between the two visibly conflicting values given for $\text{Sn}_2\text{P}_2\text{S}_6$ (20 and 190 K/GPa, respectively). Let us note that the similar data for the $x = 0.2$ solid solution crystals (cross symbols, Ref. 27) and the $x = 0.05$ solid solution crystals (Ref. 27, not included in Fig. 7), suggest already a quite narrow range of the IC phase, which seems to be much more consistent with the narrow IC phase for $\text{Sn}_2\text{P}_2\text{S}_6$ (scenario C). The latter tendency could be also easily associated with the fact that the IC phase temperature range width is strongly decreasing with the S/Se ratio at ambient pressure (see Fig. 1). Nevertheless, the phase stability of the IC phase is a strongly nonlinear function of the Se concentration at ambient pressure (see Fig. 1) and so it could be a nonmonotonous function of the Se concentration at higher pressures.

In spite of these disagreements about the temperature range of the IC phase in $\text{Sn}_2\text{P}_2\text{S}_6$, results of Ref. 28 (scenario C) and Refs. 36 and 45 (scenario B) agree well about its onset at about 0.18 GPa, $T = 296$ K. This location of the LP appears to be fairly well consistent with T - p coordinates of LPs reported for the several solid solutions with different Se concentrations (LPs are denoted by star symbols in Fig. 7). Likewise, the “theoretical” LP of the $\text{Sn}_2\text{P}_2\text{Se}_6$ compound, obtained by extrapolating of the experimental paraelectric-IC and the IC-ferroelectric phase transition temperatures towards negative pressure values (see Fig. 7), seems to lie on a more or less straight line in the projected T - p diagram.

B. Elimination of scenario B by continuity arguments

So how credible is the outcome of the present result with respect to the previous experiments? Perhaps the most significant advantage of the present experiment is that here we employed a scattering technique, which allows us to appreciate the amplitude of the order parameter as well as its wave vector. In particular, it is important that our experiments positively prove that the zone-center ferroelectric order parameter vanishes at temperatures given in Table I in a fairly continuous manner. It is well known that virtually all displacement-type IC dielectrics obey the standard continuity paradigm supported by the Landau theory:¹⁰ (i) the phase transition from the paraelectric to the IC phase is a continuous transition, and (ii) the modulated-ferroelectric “lock-in” transition is a first-order phase transition but with a relatively moderate jump of the modulation amplitude. Thus, already from these results, there is no space for an IC phase above temperatures given in Table I. Based on this argument, we can safely refute the phase diagram with a broadly opened IC phase^{36,45} (scenario B).

In order to make our conclusion even more convincing, let us recall that the atomic positions \mathbf{r}_j in the vicinity of the ferroelectric structural transition can be approximately expressed through the paraelectric reference ones ($\mathbf{r}_{j,\text{para}}$) by means of the frozen order-parameter amplitude η and corresponding eigenvector \mathbf{e}_j as

$$\mathbf{r}_j = \mathbf{r}_{j,\text{para}} + \eta \mathbf{e}_j. \quad (1)$$

Inserting this into the standard expression for the elastic neutron scattering structure factor

$$F(\mathbf{Q}) = \sum_j b_j e^{i\mathbf{Q}\cdot\mathbf{r}_j} e^{-W_j}, \quad (2)$$

where b_j is the neutron scattering length, W_j is the Debye-Waller factor of the j th atom, and \mathbf{Q} is the scattering vector and keeping the leading term in η , one obtains the reliable and frequently exploited relation

$$F(\eta, \mathbf{Q}) \approx F(0, \mathbf{Q})(1 + i\eta \mathbf{Q} \cdot \mathbf{e}_j). \quad (3)$$

This expression implies that the order parameter is modifying the elastic coherent neutron scattering intensity as

$$\begin{aligned} I(\eta, \mathbf{Q}) &= F(\eta, \mathbf{Q}) \cdot F(\eta, \mathbf{Q})^* \\ &= I(0, \mathbf{Q}) + \eta^2 I(0, \mathbf{Q}) |\mathbf{Q} \cdot \mathbf{e}_j|^2. \end{aligned} \quad (4)$$

Thus, the extraneous contribution to the Bragg reflection intensity is proportional to the square of the ferroelectric order-parameter amplitude (η^2). Moreover, it can be shown that for a long-wavelength IC phase of type II the second term in the above expression also quite well approximates the satellite reflection intensity. Consequently, the intensity by which the principal reflection is increased just below the lock-in transition should be comparable to the intensity of the satellite reflection just above the lock-in transition.

In other words, one may expect that above the lock-in phase transition, the satellite reflection in the vicinity of the $(\bar{2}00)$ Bragg reflection should have about the same intensity as the order-parameter-related part of the $(\bar{2}00)$ Bragg reflection intensity itself. Here in our measurements (see Fig. 3) the anomalous intensity of the $(\bar{2}00)$ Bragg reflection decreases considerably and *continuously* as the temperature approaches the transition temperature (given in Table I) from below, and thus we know that the order parameter vanishes there completely. This suggests that such transition cannot be a lock-in transition, and a modulated phase persisting above this temperature as proposed from the diagram of Refs. 36 and 45 (scenario B) can hardly be expected.

C. Comparison of scenarios of A and C

Therefore, the only possibility on how to reconcile our observation with a hypothesis of an IC phase is to assume that it exists *below* the transition temperatures of Table I. This could happen for a modulation wave vector smaller than the momentum resolution, as then the satellite reflection intensity would be integrated into the $(\bar{2}00)$ Bragg reflection scattering. Since a systematic broadening of the $(\bar{2}00)$ Bragg reflection was not noticed in our experiments, it would mean that the modulation period is of the order of 100 nm. The phase transition temperature of Table I would correspond to a paraelectric-IC phase transition T_i . This is in an acceptable agreement with phase transition temperatures given by Ref. 28 (scenario C).

From the same work,²⁸ one may infer that the lock-in transitions $T_{\text{lock-in}}$ would fall at about 3 K (5 K) below T_i at 0.3 GPa (at 0.6 GPa). Obviously a small jump of the order-parameter amplitude at these temperatures can hardly be identified in our data. In principle, this scenario seems to be compatible also with the birefringence data in Ref. 37.

There are indeed tiny jumps in the temperature dependence of the anomalous part of the birefringence of $\text{Sn}_2\text{P}_2\text{S}_6$ at high pressures, even though the data alone were not considered as significant.³⁷ At the same time, very similar jumps were observed at the well established $T_{\text{lock-in}}$ temperature in the temperature dependence of the birefringence data of $\text{Sn}_2\text{P}_2\text{Se}_6$, and they are also quite small,^{46–48} despite a much broader range of the IC phase there and presumably more abrupt lock-in transition. Let us note that in contrast, the compressibility data of Ref. 28 show a larger anomaly at the presumed $T_{\text{lock-in}}$ transition, while T_i is barely noticeable. The compressibility anomalies, however, do not directly scale with the order-parameter amplitude. On the contrary, it is likely that the compressibility anomalies are sensitive to the modulation period, similarly as it was demonstrated for example in the case of modulated phases of BCCD.⁴⁹ Therefore, the large compressibility anomaly at $T_{\text{lock-in}}$ might be compatible with scenario C as well.

Several possible experimental problems that might be at the origin of the contradictory reports on the splitting of the phase transition in $\text{Sn}_2\text{P}_2\text{S}_6$ have been recently discussed for example in Ref. 37. Perhaps the most serious is the peculiar sensitivity of $\text{Sn}_2\text{P}_2(\text{Se}_x\text{S}_{1-x})_6$ solid solutions to the absorption of light. It was reported that an $x = 0.2$ crystal irradiated by 0.5 W krypton (647 nm) laser radiation shows two close anomalies in the temperature dependence of the light transmission even though the crystal with this composition has nominally a single continuous phase transition.⁵⁰ We speculate that this partly understood photovoltaic or photoelastic phenomenon could be responsible for the extraneous anomalies that are behind scenario B (experiments reported in Ref. 36). However, strictly speaking, same worries apply to the experiments supporting the narrow IC phase (scenario C).

D. Order-parameter fluctuations

Additional support for scenario A can be derived from the observations of the temperature dependence of the critical fluctuations of the order parameter. In displacive ferroelectrics, the intensity of the associated quasielastic diffuse scattering is typically proportional to $1/\omega_{\text{SM}}^4$, where ω_{SM} is the soft mode frequency at a given wave vector. Therefore, the increase of the critical scattering in the vicinity of the phase transition is directly associated with soft branch frequency lowering. In the incommensurate phase, the soft mode branch is split into two branches, called phason branch and amplitudon branch, respectively.^{10,51} Obviously the diffuse scattering is mainly determined by the lower frequency phason branch.⁵² Since for small modulation amplitudes the phason gap remains zero, the phason branch and the diffuse scattering do not show much temperature evolution within the range of incommensurate phase.^{10,51,52}

The critical quasielastic diffuse scattering observed within a few degrees above the phase transition in present experiments (at 0.6 GPa, see Figs. 4 and 6) can be indeed well understood as due to an overdamped soft mode branch. In particular, the pronounced temperature dependence of the diffuse scattering intensity shown in Fig. 6(b) (data corresponding to the right-hand side scale) suggests soft mode frequency lowering upon approaching the nominal transition temperature from above.

Such temperature dependence is typical for a paraelectric phase, but not for an incommensurate phase. At the same time, the steep intensity drop below T_C suggests marked stiffening of the soft mode frequency. This can be indeed expected for a ferroelectric phase transition with a partial order-disorder character (see discussion in Refs. 53 and 54) and it is in agreement with direct measurements of both the static dielectric permittivity temperature dependence and the soft-mode frequency temperature dependence (Ref. 55) near the ambient-pressure phase transition of $\text{Sn}_2\text{P}_2\text{S}_6$.

As already mentioned, the quasielastic, that is, dynamical nature of this diffuse scattering intensity, is apparent from Fig. 6(a). Spectra taken in the immediate vicinity of T_C suggest a bell-shaped quasielastic intensity component with FWHM of the order of 0.2 THz, that is, visibly exceeding the instrumental energy resolution. Dynamic critical fluctuations with relaxational frequencies of the order of 0.2 THz would fit quite well with typical relaxation frequencies expected for soft mode fluctuations in the system (for an overdamped soft phonon mode, the relaxational frequency is about $\omega_{\text{SM}}^2/\gamma_{\text{SM}}$, where γ_{SM} is the damping of the soft phonon mode). Moreover, the quasielastic signal which for temperatures near T_C would reach the values of the order of 1000 counts at zero-energy transfer in Fig. 6(a) (extrapolation of full symbols to zero energy) does match quite nicely the 200 counts/min of the q -dependent and T -dependent diffuse signal apparent from Figs. 4 and 6(b). Thus, in brief, all the observations considered here are in a rather good agreement with the scenario of a simple paraelectric-ferroelectric phase transition (scenario A).

E. Critical behavior of the order parameter

There has been considerable interest in theoretical understanding of the critical behavior of uniaxial ferroelectrics near the TCLP and many previous studies analyzed phase transition anomalies of $\text{Sn}_2\text{P}_2\text{S}_6$ and derived solid solutions with the hope to determine the critical exponents relevant to its unconventional universality class. Since the T - p phase diagram itself is far from being established, we did not try to enter into the problem of the critical phenomena. Nevertheless, for the sake of comparison with other studies, we have analyzed our order-parameter data with the usually assumed power-law dependence on the reduced temperature $\tau = (T_C - T)/T_C$. Interestingly, the critical exponent β obtained from the adjustment of formula (4) with $\eta \propto \tau^\beta$ to the experimental data (see Fig. 3) was substantially lower than the mean-field

TABLE II. List of critical dimensions d_u and critical exponents for uniaxial ferroelectrics according to Refs. 22 and 23. The star symbol * indicates the logarithmic corrections in the power laws. (U is uniaxial dipolar, L is Lifshitz, T is tricritical, and m is dimensions of Lifshitz subspace.)

| System | d_u | α | β | γ | x |
|--------------|----------------|-----------------|-----------------|----------|----------------|
| U | 3 | 0* | $\frac{1}{2}$ * | 1* | $\frac{1}{3}$ |
| T | 3 | $\frac{1}{2}$ * | $\frac{1}{4}$ * | 1* | $\frac{1}{3}$ |
| UT | $2\frac{1}{2}$ | $\frac{1}{2}$ | $\frac{1}{4}$ | 1 | – |
| ULT, $m = 1$ | 3 | $\frac{1}{2}$ * | $\frac{1}{4}$ * | 1* | $\frac{1}{10}$ |

value of 0.5. This result is in contradiction with the analysis of Refs. 29 and 30. On the other hand, our values of β measured above $p_{\text{TCP}} = 0.18$ GPa are nicely joining those obtained below p_{TCP} from the spontaneous polarization (respectively pyroelectric coefficient) data of $\text{Sn}_2\text{P}_2(\text{Se}_{0.04}\text{S}_{0.96})_6$.²⁷ Moreover, by far the best fit [see Fig. 3(a)] was obtained for adjustment to the expected logarithm-corrected power law^{22,56,57}

$$\eta = A\tau^\beta |\ln(\tau)|^x, \quad (5)$$

with $\beta = 1/4$ and $x = 1/10$, that is, values imposed according to the predictions for the critical behavior in the vicinity of a TCLP of a uniaxial ferroelectric²² (see Table II).

V. CONCLUSION

In conclusion, this paper clarifies the nature of the ferroelectric phase transition in the $\text{Sn}_2\text{P}_2\text{S}_6$ single crystal under a moderate hydrostatic pressure (up to 0.6 GPa). The neutron diffraction experiments indicate clearly that the ferroelectric order parameter vanishes in a fairly continuous manner at a well-resolved transition temperature. In spite of considerable efforts, no evidence of an intermediate incommensurate phase was obtained. While we cannot fully exclude the existence of an extremely long-wavelength modulation below the phase

transition temperature, the most simple explanation of our observations is that at least up to 0.6 GPa, there is only a simple paraelectric-ferroelectric phase transition in $\text{Sn}_2\text{P}_2\text{S}_6$. Still, the temperature dependence of the order parameter happens to be best reproduced by the logarithm-corrected power law expected for a uniaxial ferroelectric system in the vicinity of a TCLP. Thus, it is quite possible that the thermodynamical properties of the $\text{Sn}_2\text{P}_2\text{S}_6$ compound and derived solid solutions may reflect the theoretical closeness to the ideal TCLP behavior and so it should be taken into account in analysis of the data.

ACKNOWLEDGMENTS

The work was partly supported by the Grant Agency of the Czech Republic (Projects No. P204/10/0616 and No. 202/09/H041) and by Project No. SVV-2012-265307. Y.V. is grateful for the support during the visit to LLB, and all authors thank François Maignen, Stéphane Pailhès, and Patrick Baroni for technical supports at LLB. K.Z.R. gratefully acknowledges past support from the Alexander von Humboldt Foundation, Germany, and current support from the Young Investigators Group Programme of the Helmholtz Association, Germany, contract VH-NG-409.

-
- ¹S. Lee, J. A. Bock, S. Trolier-McKinstry, and C. A. Randall, *J. Eur. Ceram. Soc.* **32**, 3971 (2012).
- ²S. Y. Yang, J. Seidel, S. J. Byrnes, P. Shafer, C.-H. Yang, M. D. Rossell, P. Yu, Y.-H. Chu, J. F. Scott, J. W. Ager III, L. W. Martin, and R. Ramesh, *Nat. Nanotechnol.* **5**, 143 (2010).
- ³J. Seidel, D. Fu, S.-Y. Yang, E. Alarcón-Lladó, J. Wu, R. Ramesh, and J. W. Ager III, *Phys. Rev. Lett.* **107**, 126805 (2011).
- ⁴J. W. Bennett, K. F. Garrity, K. M. Rabe, and D. Vanderbilt, *Phys. Rev. Lett.* **109**, 167602 (2012).
- ⁵D. Daranciang, M. J. Highland, H. Wen, S. M. Young, N. C. Brandt, H. Y. Hwang, M. Vattilana, M. Nicoul, F. Quirin, J. Goodfellow, T. Qi, I. Grinberg, D. M. Fritz, M. Cammarata, D. Zhu, H. T. Lemke, D. A. Walko, E. M. Dufresne, Y. Li, J. Larsson, D. A. Reis, K. Sokolowski-Tinten, K. A. Nelson, A. M. Rappe, P. H. Fuoss, G. B. Stephenson, and A. M. Lindenberg, *Phys. Rev. Lett.* **108**, 087601 (2012).
- ⁶M. Imlau, V. Dieckmann, H. Badorreck, and A. Shumelyuk, *Opt. Mater. Express* **1**, 953 (2011).
- ⁷D. Tiwari and S. Dunn, *J. Mater. Sci.* **44**, 5063 (2009).
- ⁸J. W. Bennett and K. M. Rabe, *J. Solid State Chem.* **195**, 21 (2012).
- ⁹Yu. M. Vysochanskii, T. Janssen, R. Currat, R. Folk, J. Banys, J. Grigas, and V. Samulionis, *Phase Transitions in Phosphorous Chalcogenide Ferroelectrics* (Vilnius University, Vilnius, 2006).
- ¹⁰R. Blinc and A. P. Levanyuk, *Incommensurate Phases in Dielectrics*, Vol. 1 (North-Holland, Amsterdam, 1986).
- ¹¹S. W. H. Eijt, R. Currat, J. E. Lorenzo, P. Saint-Gregoire, B. Hennion, and Yu. M. Vysochanskii, *Eur. Phys. J. B* **5**, 169 (1998).
- ¹²H. W. Diehl, M. A. Shtpot, and R. K. P. Zia, *Phys. Rev. B* **68**, 224415 (2003).
- ¹³K. Z. Rushchanskii, Yu. M. Vysochanskii, and D. Strauch, *Phys. Rev. Lett.* **99**, 207601 (2007).
- ¹⁴A. Kohutych, R. Yevych, S. Perechinskii, V. Samulionis, J. Banys, and Yu. M. Vysochanskii, *Phys. Rev. B* **82**, 054101 (2010).
- ¹⁵A. Oleaga, A. Salazar, A. A. Kohutych, and Yu. M. Vysochanskii, *J. Phys.: Condens. Matter* **23**, 025902 (2011).
- ¹⁶V. Yu. Korda, S. V. Berezovsky, A. S. Molev, L. P. Korda, and V. F. Klepikov, *Physica B* **407**, 3388 (2012).
- ¹⁷A. N. Morozovska, E. A. Eliseev, J. J. Wang, G. S. Svechnikov, Yu. M. Vysochanskii, V. Gopalan, and L.-Q. Chen, *Phys. Rev. B* **81**, 195437 (2010).
- ¹⁸A. V. Gomonnai, A. A. Grabar, Y. M. Vysochanskii, A. D. Belyayev, V. F. Machulin, M. I. Gurzan, and V. Y. Slivka, *Fiz. Tverd. Tela (Leningrad)* **23**, 3602 (1981) (in Russian).
- ¹⁹C. D. Carpentier and R. Nitsche, *Mater. Res. Bull.* **9**, 1097 (1974).
- ²⁰T. K. Barsamian, S. S. Khasanov, V. Sh. Shekhtman, Yu. M. Vysochanskii, and V. Yu. Slivka, *Ferroelectrics* **67**, 47 (1986).
- ²¹R. Israel, R. de Gelder, J. M. M. Smits, P. T. Beurskens, S. W. H. Eijt, Th. Rasing, H. van Kempen, M. M. Maior, and S. F. Motrija, *Z. Kristall.* **213**, 34 (1998).
- ²²R. Folk and G. Moser, *Phys. Rev. B* **47**, 13992 (1993).
- ²³R. Folk, *Phase Trans.* **67**, 645 (1999).
- ²⁴Yu. M. Vysochanskii, V. G. Furtsev, M. M. Khoma, A. A. Grabar, M. I. Gurzan, M. M. Maior, S. I. Perechinskii, V. M. Rizak, and V. Yu. Slivka, *Zh. Eksp. Teor. Fiz.* **91**, 1384 (1986) [*Sov. Phys. JETP* **64**, 816 (1986)].
- ²⁵Yu. M. Vysochanskii and V. Yu. Slivka, *Sov. Phys. Usp.* **35**, 123 (1992).
- ²⁶O. Andersson, O. Chobal, I. Rizak, and V. Rizak, *Phys. Rev. B* **80**, 174107 (2009).
- ²⁷A. G. Slivka, E. I. Gerzanich, P. P. Guranich, and V. S. Shusta, *Ferroelectrics* **103**, 71 (1990).

- ²⁸A. G. Slivka, E. I. Gerzanich, P. P. Guranich, V. S. Shusta, and V. M. Kedyulich, *Condens. Matter Phys.* **2**, 415 (1999).
- ²⁹P. P. Guranich, R. V. Kabal, A. G. Slivka, and E. I. Gerzanich, *Ukr. J. Phys. Opt.* **2**, 179 (2001).
- ³⁰P. P. Guranich, A. G. Slivka, V. S. Shusta, O. I. Gerzanich, and I. Yu. Kuritsa, *Ferroelectrics* **316**, 177 (2005).
- ³¹E. I. Gerzanich, *Ukr. J. Phys. Opt.* **9**, 129 (2008).
- ³²See Fig. 1 in Ref. 27.
- ³³B. Zapeka, O. Mys, and R. Vlokh, *Ferroelectrics* **418**, 143 (2011).
- ³⁴Yu. M. Vysochanskii, M. M. Mayor, V. M. Rizak, V. Yu. Slivka, and M. M. Khoma, *Zh. Eksp. Teor. Fiz.* **95**, 1355 (1989) [*Sov. Phys. JETP* **68**, 782 (1989)].
- ³⁵Yu. M. Vysochanskii, A. A. Kohutych, A. V. Kityk, A. V. Zadorozhna, M. M. Khoma, and A. A. Grabar, *Ferroelectrics* **399**, 83 (2010).
- ³⁶Yu. Tyagur, E. I. Gerzanich, and A. G. Slivka, *Sov. Phys. J.* **28**, 739 (1985).
- ³⁷A. Say, O. Mys, D. Adamenko, A. Grabar, Y. Vysochanskii, A. Kityk, and R. Vlokh, *Phase Trans.* **83**, 123 (2010).
- ³⁸G. Dittmar and H. Schafer, *Z. Naturforsch. B* **29**, 312 (1974).
- ³⁹B. Scott, M. Pressprich, R. D. Willet, and D. A. Cleary, *J. Solid State Chem.* **96**, 294 (1992).
- ⁴⁰S. W. H. Eijt, R. Currat, J. E. Lorenzo, P. Saint-Gregoire, S. Katano, T. Janssen, B. Hennion, and Yu. M. Vysochanskii, *J. Phys.: Condens. Matter* **10**, 4811 (1998).
- ⁴¹T. K. Barsamian, S. S. Khasanov, and V. Sh. Shekhtman, *Ferroelectrics* **138**, 63 (1993).
- ⁴²V. Petricek, M. Dusek, and L. Palatinus, Jana2006, the crystallographic computing system. Institute of Physics AS CR, Prague, Czech Republic (2006).
- ⁴³J. Hlinka, R. Currat, M. de Boissieu, F. Livet, and Yu. M. Vysochanskii, *Phys. Rev. B* **71**, 052102 (2005).
- ⁴⁴A. G. Slivka, V. M. Kedyulich, and E. I. Gerzanich, *Ferroelectrics* **317**, 89 (2005).
- ⁴⁵O. Andersson, O. Chobal, I. Rizak, V. Rizak, and V. Sabadosh, *Phys. Rev. B* **83**, 134121 (2011).
- ⁴⁶Yu. M. Vysochanskii, S. F. Motrja, S. I. Perechinskii, V. M. Rizak, I. M. Rizak, and V. Yu. Slivka, *Ukr. Fiz. Zh.* **36**, 728 (1991).
- ⁴⁷See Ref. 9, Fig. 3.25, p. 167.
- ⁴⁸I. M. Rizak, V. M. Rizak, S. I. Perechinskii, Yu. M. Vysochanskii, and V. Yu. Slivka, *Ferroelectrics* **143**, 67 (1993).
- ⁴⁹J. Hlinka, M. Iwata, and Y. Ishibashi, *J. Phys. Soc. Jpn.* **68**, 126 (1999).
- ⁵⁰Yu. M. Vysochanskii, V. G. Furtsev, M. M. Khoma, M. I. Gurzan and V. Yu. Slivka, *Zh. Eksp. Teor. Fiz.* **89**, 939 (1985) [*Sov. Phys. JETP* **62**, 540 (1985)].
- ⁵¹R. Currat and T. Janssen, *Solid State Phys.* **41**, 201 (1988).
- ⁵²J. Hlinka, J. Petzelt, B. Brezina, and R. Currat, *Phys. Rev. B* **66**, 132302 (2002).
- ⁵³J. Hlinka, T. Janssen, and V. Dvorak, *J. Phys.: Condens. Matter* **11**, 3209 (1999).
- ⁵⁴S. Padlewski, A. K. Evans, C. Ayling, and V. Heine, *J. Phys.: Condens. Matter* **4**, 4895 (1992).
- ⁵⁵A. A. Volkov, G. V. Kozlov, N. I. Afanas'eva, Yu. M. Vysochanskii, A. A. Grabar, and V. Yu. Slivka, *Sov. Phys. Solid State* **25**, 1482 (1983).
- ⁵⁶A. I. Larkin and D. E. Khmel'nitskii, *Zh. Eksp. Teor. Fiz.* **56**, 2087 (1969) [*Sov. Phys. JETP* **29**, 1123 (1969)].
- ⁵⁷A. Aharony, *Phys. Rev. B* **8**, 3363 (1973).